Stability of explicit numerical schemes for convection-dominated problems

Erwan Deriaz* and Dmitry Kolomenskiy*

July 20, 2010

Abstract

Operating a refined von Neumann stability analysis of the transport equation, we demonstrate why some explicit schemes involve a CFL-like stability condition of the type $\delta t \leq C\delta x^{2r/(2r-1)}$ with δt the time step, δx the space step and r an integer, when applied to convection dominated problems.

keywords: CFL condition, von Neumann stability, transport equation, Navier-Stokes equation, Runge-Kutta schemes.

1 Introduction

In numerical fluid mechanics, many simulations for transport-dominated problems employ explicit second order time discretization schemes, either of Runge-Kutta type [8, 6] or Adams-Bashforth [10, 11] (see equations (5.42), (5.43), (5.46)). Although widely in use and proved efficient, the stability domains of these order two numerical schemes (see fig 1) exclude the (Oy) axis corresponding to transport problems. Nonetheless, actual experiments [18, 6] show that even in this case, a convergent solution can be obtained. If the problem admits a sufficiently smooth, classical solution, the second order time-stepping is stable at worst under a condition of type $\delta t_{\max} \leq C(\delta x/u_{\max})^{4/3}$, where δt is the time step, δx the space step, and $u_{\max}$ the maximum velocity of the transport problem.

A close look at the von Neumann stability criterion applied to transport equation provides an explanation. To the best of our knowledge, this result is new –for instance, it is not presented in [17] which has collected the state of the art in numerical stability– despite its simplicity and the fact that it applies to a wide variety of numerical problems. Under some smoothness conditions, it readily extends to Burgers equation, incompressible Euler equations, Navier-Stokes equations with a high Reynolds number on any domains possibly bounded with walls, and more generally to conservation laws.

For the single step numerical method (i.e. the explicit Euler scheme), a stability result relying on a similar approach and providing a stability constraint of the type $\delta t_{\max} \leq C(\delta x/u_{\max})^2$ has been presented by several authors [13, 9, 15]. This stability condition originates from a completely different kind of numerical instability than the usual stability condition for the heat equation with explicit schemes. As we will see in this article, the power two comes from the order of tangency of the stability domain to the (Oy) axis. Actually, we present here the generalization of this stability constraint. Moreover, we

*Laboratoire de Mécanique, Modélisation et Procédés Propres, 38 rue Frédéric Joliot-Curie 13451 MARSEILLE Cedex 20 (France), erwan.deriaz@l3m.univ-mrs.fr, dkolom@l3m.univ-mrs.fr

make a direct connection between the order of the numerical method and its stability for transport dominated problems.

As the numerical viscosity may stabilize the time scheme, this criterion applies essentially to pseudo-spectral methods and numerical methods with high order in space [18]. The numerical experiments allow us to validate our approach very accurately.

The paper is organized as follows: first we recall the definition and the computation of the von Neumann stability; then we make accurate computations for the linear transport problem predicting a Courant-Friedrichs-Lewy condition of the type $\delta t_{\leq} C(\delta x/u)^{2r/(2r-1)}$ with r an integer; then we construct numerical schemes giving such a stability condition with $r = 1, 2, 3, 4$, that means exponents equal to 2, $\frac{4}{3}$, $\frac{6}{5}$ and $\frac{8}{7}$; finally we show how this stability criterion extends to non-linear equations.

2 The von Neumann stability condition

Let us consider the equation

$$\partial_t u = F(u) \tag{2.1}$$

where $u : \mathbb{R}^d$ or $\mathbb{T}^d \to \mathbb{R}$ and F is a linear operator. We define $\sigma(\boldsymbol{\xi})$ as the constant symbol corresponding to F, i.e. $\widehat{F(u)}(\boldsymbol{\xi}) = \sigma(\boldsymbol{\xi})\widehat{u}(\boldsymbol{\xi})$.

We study the stability of temporal discrete schemes applied to such a differential equation using the von Neumann method. We do not take into account the spacial discretization. It means we consider we have a spectral discretization, or that the $F(u_k)$ terms are orthogonally reprojected in our discretization space. The time integration schemes can be of Runge-Kutta type:

$$u_{(0)} = u_n, \quad u_{(\ell)} = \sum_{i=0}^{\ell-1} a_{\ell i}\, u_{(i)} + \delta t \sum_{i=0}^{\ell-1} b_{\ell i}\, F(u_{(i)}) \ \text{ for } 1 \leq \ell \leq s', \quad u_{n+1} = u_{(s')} \tag{2.2}$$

where δt is the time step, for some $(a_{\ell i})_{\ell,i}$ and $(b_{\ell i})_{\ell,i}$ well chosen to ensure the accuracy of the integration.

Or they can be of explicit multi-step (Adams-Bashforth) type:

$$u_{n+1} = \sum_{i=0}^{s} c_i\, u_{n-i} + \delta t \sum_{i=0}^{s} d_i\, F(u_{n-i}) \tag{2.3}$$

We can also mix these two types of integration schemes:

$$u_{(\ell)} = \sum_{i=1}^{\ell-1} a_{\ell i}\, u_{(i)} + \sum_{i=0}^{s} c_{\ell i}\, u_{n-i} + \delta t \sum_{i=0}^{\ell-1} b_{\ell i}\, F(u_{(i)}) + \delta t \sum_{i=0}^{s} d_i\, F(u_{n-i}) \text{ for } 1 \leq \ell \leq s',$$
$$u_{n+1} = u_{(s')} \tag{2.4}$$

We isolate a Fourier mode $\boldsymbol{\xi}$ by taking $u_n(\mathbf{x}) = \phi_n\, e^{i\boldsymbol{\xi}\cdot\mathbf{x}}$. Actually, if δx is the space step, then $0 \leq \xi_\ell \leq \frac{\pi}{\delta x}$ for $1 \leq \ell \leq d$.

In the case several previous time samples are necessary, like in Adams-Bashforth type schemes, we put

$$X_n = \begin{pmatrix} u_n \\ u_{n-1} \\ \vdots \\ u_{n-s} \end{pmatrix} \tag{2.5}$$

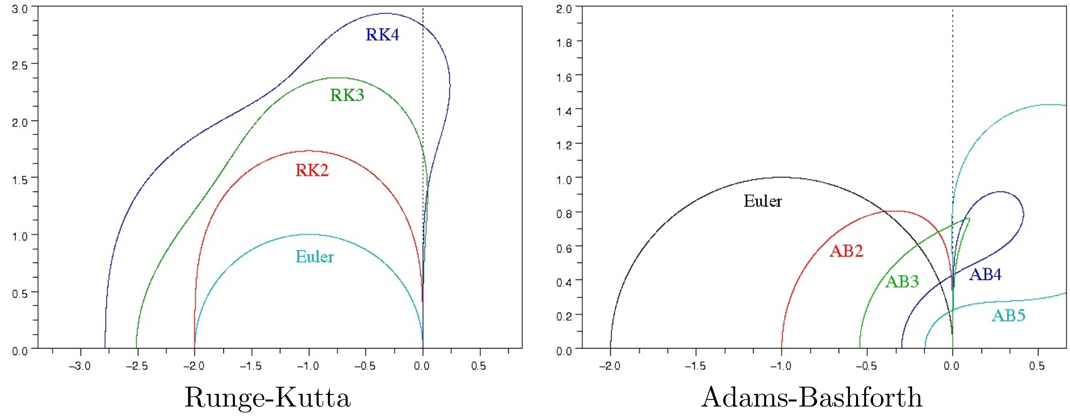

Figure 1: Von Neumann stability domains for Runge-Kutta and Adams-Bashforth schemes.

Then for the specific Fourier mode $\boldsymbol{\xi}$, seeing that each time we apply F to a term, we also multiply this term by δt, relation (2.4) provides

$$X_{n+1} = M(\sigma(\boldsymbol{\xi})\delta t)X_n \tag{2.6}$$

where, putting $\boldsymbol{\zeta} = \sigma(\boldsymbol{\xi})\delta t$, $M(\boldsymbol{\zeta})$ is a $(s+1) \times (s+1)$ square matrix. Note that $\xi_\ell \delta t \in [0, \pi\frac{\delta t}{\delta x}]$. Let $\lambda_0(\boldsymbol{\zeta}), \ldots, \lambda_s(\boldsymbol{\zeta})$ be the eigenvalues of $M(\boldsymbol{\zeta})$, and the spectral radius $\rho(M(\boldsymbol{\zeta})) = \max_{0\leq i\leq s}|\lambda_{k_i}(\boldsymbol{\zeta})|$, then $\rho(M(\boldsymbol{\zeta}))^n \leq \|M(\boldsymbol{\zeta})^n\| \leq \|M(\boldsymbol{\zeta})\|^n$, and for almost every $M(\boldsymbol{\zeta})$, $\exists K(M(\boldsymbol{\zeta})) > 0$, $\forall n \geq 0$, $\|M(\boldsymbol{\zeta})^n\| \leq K(M(\boldsymbol{\zeta}))\rho(M(\boldsymbol{\zeta}))^n$ where the constant $K(M(\boldsymbol{\zeta}))$ becomes large near the singularities (see [15]). Hence the von Neumann stability of the scheme (2.4) boils down to

$$\forall i, \boldsymbol{\zeta}, \quad |\lambda_i(\boldsymbol{\zeta})| \leq 1 + C\delta t \tag{2.7}$$

with C a positive constant independent of δx and δt. Sometimes, C is taken equal to zero to enforce a better stability. The assumption (2.7) allows any error ε_0 to stay bounded after a time elapse T, since

$$\|\varepsilon_T\| = \|M(\boldsymbol{\zeta})^{T/\delta t}\varepsilon_0\| \leq K(M(\boldsymbol{\zeta}))(1 + C\delta t)^{T/\delta t}\|\varepsilon_0\| \leq K(M(\boldsymbol{\zeta}))e^{CT}\|\varepsilon_0\| \tag{2.8}$$

The von Neumann stability domain of the temporal scheme (2.4) is given by $\{\boldsymbol{\zeta} \in \mathbb{C}^d, \rho(M(\boldsymbol{\zeta})) \leq 1\}$. In figures 1, 2, 3, $d = 1$ so the x-axis represents the real part of ζ and the y-axis its imaginary part.
We plot this domain by plotting all the curves (hypersurfaces) $\{\boldsymbol{\zeta} \in \mathbb{C}^d, |\lambda_\ell(\boldsymbol{\zeta})| \leq 1\}$ taking $\lambda_\ell(\boldsymbol{\zeta}) = e^{i\theta}$, $\theta \in [0, 2\pi[$, for $0 \leq \ell \leq s$. The stability domain is delimited by these curves.
On figure 1 we plotted an example for such domains for the four first Runge-Kutta integration schemes and the five first Adams-Bashforth schemes. Actually the lines correspond to all the values ζ of the operator $\delta t\, F$ for which there exists an eigenvalue with modulus equal to one. So the stability domain only corresponds to the inner semi-disk near zero. In particular for orders four and five, the loops on the right do not correspond to any stable domain.

The behavior of the stability domain along the axis (Oy) indicates how the temporal scheme will be stable under the condition $\rho(M(\boldsymbol{\zeta})) \leq 1 + C\delta t$ –which gives more relevant stability conditions than $\rho(M(\boldsymbol{\zeta})) \leq 1$– for convection-dominated problems. The next parts of our study will be dedicated to finding precise stability conditions on δt and δx in the frame of von Neumann stability, and show that these results extend to regular solutions of non-linear problems such as the incompressible Euler equations or the Navier-Stokes equations when the Reynolds number is large, on a domain Ω bounded with walls.

3 Stability conditions for the transport equation

In this section, we present accurate computations for the transport equation, and apply the results to some popular schemes in fluid dynamics. When we simplify the transport problem to reduce it to its most basic expression, we have the equation

$$\partial_t u + a\,\partial_x u = 0 \tag{3.1}$$

Since $\widehat{f'}(\xi) = i\xi \widehat{f}(\xi)$, the symbol of the $F(u) = -a\,\partial_x u$ is equal to: $\sigma(\xi) = -i\,a\,\xi$.
As explained in the previous section, taking $u_n(\mathbf{x}) = \phi_n\, e^{i\,\xi\,x}$, and putting X_n as in equation (2.6), we can write:

$$X_{n+1} = A(\xi)X_n \tag{3.2}$$

with A a matrix whose coefficients are polynomials in $-i\,a\,\xi\,\delta t$.
In the case the numerical scheme is of Runge-Kutta type, then $A(\xi)$ is a polynomial:

$$A(\xi) = \sum_{\ell=0}^{s} \beta_\ell (-i\,a\,\xi)^\ell \delta t^\ell \tag{3.3}$$

The coefficients (β_ℓ) of this polynomial play an important role in our stability analysis. We are able to compute the norm of $A(\xi)$ explicitly:

$$|A(\xi)|^2 = \sum_{\ell=0}^{s} S_\ell \delta t^{2\ell} a^{2\ell} \xi^{2\ell} \tag{3.4}$$

with, assuming $\beta_j = 0$ for $j > s$,

$$S_\ell = \sum_{j=0}^{2\ell} (-1)^{\ell+j} \beta_j \beta_{2\ell-j} \tag{3.5}$$

The von Neumann stability condition $|A(\xi)| \leq 1 + C\delta t$ for all ξ in the computational domain and for a given C, implies that for $\xi \in [0, \frac{1}{\delta x}]$, (usually the computational domain is rather $[0, \frac{\pi}{\delta x}]$, but we discard π for simplicity):

$$\sum_{\ell=0}^{s} S_\ell \delta t^{2\ell} a^{2\ell} \xi^{2\ell} \leq 1 + 2C\delta t \tag{3.6}$$

For sake of consistency of the numerical scheme, $\beta_0 = 1$ so $S_0 = \beta_0^2 = 1$. Then if $S_1 = \cdots = S_{r-1} = 0$ and $S_r > 0$ for a given integer r, we can write for small ξ,

$$|A(\xi)|^2 = 1 + S_r \delta t^{2r} a^{2r} \xi^{2r} + o(\xi^{2r}) \tag{3.7}$$

and $\delta t^{2r} a^{2r} \xi^{2r} \to 0$ for $\delta t \to 0$ implies $\delta t \xi = o(1)$ i.e. as $\xi \sim 1/\delta x$, $\delta x = o(\delta t)$. Hence the equation (3.7) is valid for all the computational domain $[0, \frac{1}{\delta x}]$. And the stability condition (3.6) is reduced to:

$$S_r \delta t^{2r} a^{2r} \delta x^{-2r} \leq 2C\delta t \tag{3.8}$$

i.e.

$$\delta t \leq \left(\frac{2C}{S_r}\right)^{\frac{1}{2r-1}} \left(\frac{\delta x}{a}\right)^{\frac{2r}{2r-1}}. \tag{3.9}$$

This stability condition is directly linked to the tangency of the stability domain $\{\xi \in \mathbb{C}, |A(\xi)| \leq 1\}$ to the vertical axis (Oy). Let us write the amplification factor $g(\zeta) = A(\xi)$:

$$g(\zeta) = 1 + \zeta + \beta_2\zeta^2 + \cdots + \beta_s\zeta^s \tag{3.10}$$

where, for consistency reasons, we put $\beta_0 = \beta_1 = 1$.
Near 0, $\zeta = p + i\,q$,

$$g(\zeta) = 1 + p + iq + \beta_2(p+iq)^2 + \cdots + \beta_s(p+iq)^s \tag{3.11}$$

with p and q independent variables going to zero. Then,

$$|g(\zeta)|^2 = (1 + p + \beta_2(p^2 - q^2) + \dots)^2 + (q + 2\beta_2\, p\, q + \dots)^2. \tag{3.12}$$

The first terms appearing in this sum are 1 and $2p$, but we do not know which is the lower power of q appearing in this sum yet. Nevertheless, all the terms $p^\ell q^j$ and p^ℓ are negligible in front of p, so we have from (3.10)

$$\begin{aligned} |g(\zeta)|^2 &= |1 + p + iq + \beta_2(iq)^2 + \cdots + \beta_s(iq)^s|^2 + o(p) \\ &= 1 + 2p + S_r\, q^{2r} + o(p + q^{2r}) = 1 \end{aligned} \tag{3.13}$$

and the tangent is given for $p = -\frac{S_r}{2} q^{2r}$ i.e. by

$$\xi = -\frac{S_r}{2} q^{2r} + iq, \quad q \in \mathbb{R}. \tag{3.14}$$

There is an equivalence between this tangency and the CFL (3.9).

This provides the following stability conditions for some of the most used schemes for transport problems:

- The simplest example is the Euler explicit scheme, order one in time:

$$u_{n+1} = u_n - \delta t\ a \nabla u_n \tag{3.15}$$

For this, $g(\zeta) = 1 + \zeta$ so $r = 1$, $S_1 = 1$ and we find the CFL condition:

$$\delta t \leq 2C \left(\frac{\delta x}{a}\right)^2 \tag{3.16}$$

- An improved version of this scheme allows us to construct an order two centered scheme:

$$\left\{\begin{array}{ll} u_{n+1/2} = & u_n - \frac{\delta t}{2} a \nabla u_n \\ u_{n+1} = & u_n - \delta t \; a \nabla u_{n+1/2} \end{array}\right. \tag{3.17}$$

For this scheme, $g(\zeta) = 1 + \zeta + \frac{1}{2}\zeta^2$ so $r = 2$ because $S_1 = 0$ and $S_2 = \frac{1}{4}$. Compared to the previous case, the stability is improved:

$$\delta t \leq 2C^{1/3} \left(\frac{\delta x}{a}\right)^{4/3} \tag{3.18}$$

- For Runge-Kutta scheme of order 4:

$$\left\{\begin{array}{ll} u_{n(1)} = & u_n - \frac{\delta t}{2} a \nabla u_n \\ u_{n(2)} = & u_n - \frac{\delta t}{2} a \nabla u_{n(1)} \\ u_{n(3)} = & u_n - \delta t \; a \nabla u_{n(2)} \\ u_{n+1} = & u_n - \frac{\delta t}{6} a \nabla u_n - \frac{\delta t}{3} a \nabla u_{n(1)} - \frac{\delta t}{3} a \nabla u_{n(2)} - \frac{\delta t}{6} a \nabla u_{n(3)} \end{array}\right. \tag{3.19}$$

computations show that actually:

$$S_1 = S_2 = 0 \quad \text{and} \quad S_3 = -\frac{1}{72},\, S_4 = \frac{1}{576} \tag{3.20}$$

Hence our study doesn't fully apply to this case.

- The order two Adams-Bashforth scheme goes as follows:

$$u_{n+1} = u_n - \frac{3}{2}\delta t \; a \nabla u_n + \frac{1}{2}\delta t \; a \nabla u_{n-1} \tag{3.21}$$

So, according to section 2, we put $X_n = \begin{bmatrix} u_n \\ u_{n-1} \end{bmatrix}$, so taking $u_n(x) = \phi_n \, e^{i\xi\, x}$, we obtain:

$$X_{n+1} = \begin{bmatrix} 1 + \frac{3}{2}\zeta & -\frac{\zeta}{2} \\ 1 & 0 \end{bmatrix} X_n \tag{3.22}$$

with $\zeta = -ia\delta t\xi$.
We compute the eigenvalue of this 2×2 matrix, the characteristic polynomial is given by $\chi(Y) = Y^2 - (1 + \frac{3}{2}\zeta)Y + \frac{\zeta}{2}$. Owing to the fact that $\delta t = o(\delta x)$, we have $\zeta \to 0$. An expansion of the larger eigenvalue Y_0 in terms of powers of ζ provides

$$Y_0 = 1 + \zeta + \frac{\zeta^2}{2} - \frac{\zeta^3}{4} - \frac{\zeta^4}{8} + o(\zeta^4) \tag{3.23}$$

With $\zeta = -ia\frac{\delta t}{\delta x}$, we obtain

$$|Y_0| = 1 + \frac{1}{4} a^4 \frac{\delta t^4}{\delta x^4} + o(\frac{\delta t^4}{\delta x^4}) \tag{3.24}$$

As we want $|Y_0| \leq 1 + C\delta t$, this drives to the following stability condition:

$$\delta t \leq 2^{2/3} C^{1/3} \left(\frac{\delta x}{a}\right)^{4/3} \tag{3.25}$$

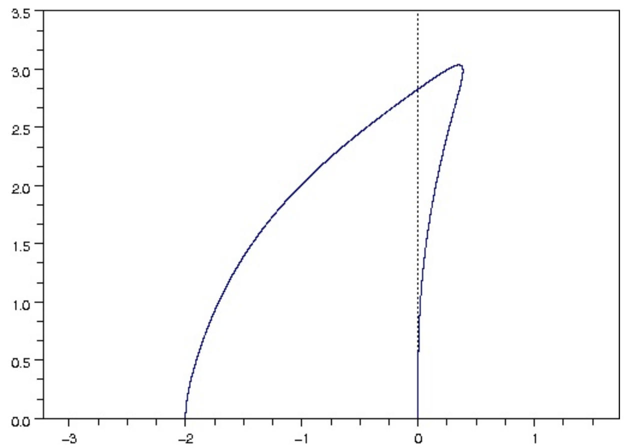

Figure 2: Von Neumann stability domain for the pseudo-Leap-Frog scheme equation (3.26).

Therefore, two popular second order schemes, Runge Kutta two (RK2) and Adams-Bashforth two (AB2) require a CFL-like condition: $\delta t \leq C\delta x^{4/3}$. As indicated in part 5.2, the $\delta t_{\max}$ is $2^{1/3}$ larger for RK2 than for AB2, but RK2 necessitates twice more computations than AB2. So, regarding only the stability, AB2 is $2^{2/3}$ cheaper than RK2.

Not all the second order numerical schemes needs to satisfy a 4/3-CFL condition. For instance, to the Leap-Frog scheme corresponds a usual linear CFL stability condition. The following second order method is also stable under a linear CFL condition:

$$\mathbf{u}_{n+1} = \mathbf{u}_n + \delta t\, F\left(\frac{\mathbf{u}_n + \mathbf{u}_{n-1}}{2} + \delta t\, F(\mathbf{u}_n)\right) \tag{3.26}$$

Its stability domain is drawn in figure 2. The fact that $r = 2$ with $S_2 < 0$ is reflected by a tangency oriented to the right.

Theorem 3.1 *An order $2p$ numerical scheme applied to the transport equation is, at worst, stable under the CFL-like condition:*

$$\delta t \leq C\left(\frac{\delta x}{a}\right)^{\frac{2p+2}{2p+1}} \tag{3.27}$$

Proof: For an order $2p$ scheme, we have:

$$u_{n+1} = u_n + \delta t\, \partial_t u_n + \frac{\delta t^2}{2}\partial_t^2 u_n + \cdots + \frac{\delta t^{2p}}{(2p)!}\partial_t^{2p} u_n + o(\delta t^{2p}) \tag{3.28}$$

As for the transport equation, F is linear, F and ∂_t commute, so iterating $\partial_t u = F(u)$ we obtain $\partial_t^\ell u_n = F^\ell(u_n)$. Hence equation (3.28) yields the amplification factor:

$$g(\zeta) = 1 + \zeta + \frac{\zeta^2}{2} + \cdots + \frac{\zeta^{2p}}{(2p)!} + o(\zeta^{2p}) \tag{3.29}$$

with $o()$ gathering the negligible terms under the condition $\delta t = o(\delta x)$. And the (β_ℓ) are given by $\beta_\ell = \frac{1}{\ell!}$. Then for $q \in [1, p]$, the coefficients S_q of the sum (3.4) are given by:

$$S_q = \sum_{\ell=0}^{2q} (-1)^{(q-\ell)} \frac{1}{\ell!} \; \frac{1}{(2q-\ell)!} = \frac{(-1)^q}{(2q)!} \sum_{\ell=0}^{2q} \mathrm{C}_{2q}^{\ell} (-1)^\ell = 0 \tag{3.30}$$

Hence, in the worst case regarding the stability, the first non zero significant term in the sum (3.4), under the condition $\delta t = o(\delta x)$, is $S_{p+1} \delta t^{2p+2} a^{2p+2} \xi^{2p+2}$ implying the stability condition (3.27).

4 Simple $2N$-storage numerical schemes with positive energy deviation

In order to illustrate the phenomenon presented in the previous section, we construct numerical schemes having stability conditions of the type $\delta t \le C \left(\frac{\delta x}{A_0}\right)^{2r/2r-1}$, and which only necessitate two time levels to be stored in the computer memory. The three schemes presented here have been constructed in order to give an example for the stability analysis leading to exponents $2r/2r-1$ different from 1. It is not advisable to use these numerical schemes due to their poor consistency. Other efficient $2N$-storage schemes can be found in [10].

To solve the equation

$$\partial_t u = F(u), \tag{4.1}$$

let us consider the following family of schemes:

$$\begin{array}{rcl} u_{n\,(0)} & = & u_n \\ u_{n\,(1)} & = & u_n + \alpha_p \delta t F(u_{n\,(0)}) \\ \dots & & \\ u_{n\,(\ell)} & = & u_n + \alpha_{p-\ell} \delta t F(u_{n\,(\ell-1)}) \\ \dots & & \\ u_{n+1} & = & u_n + \alpha_1 \delta t F(u_{n\,(p-1)}) \end{array} \tag{4.2}$$

These can also be written as:

$$u_{n+1} = u_n + \alpha_1 \delta t F(u_n + \alpha_2 \delta t F(u_n + \alpha_3 \delta t F(u_n + \dots))) \tag{4.3}$$

If F is **linear**, this corresponds to

$$u_{n+1} = u_n + \beta_1 \delta t F(u_n) + \beta_2 \delta t^2 F^2(u_n) + \beta_3 \delta t^3 F^3(u_n) + \dots \tag{4.4}$$

with $\beta_m = \prod_{\ell=1}^m \alpha_\ell$. Or, owing to $F^\ell(u) = \partial_t^\ell u$,

$$u_{n+1} = u_n + \beta_1 \delta t \partial_t u_n + \beta_2 \delta t^2 \partial_t^2 u_n + \beta_3 \delta t^3 \partial_t^3 u_n + \dots \tag{4.5}$$

Here we recognize an expansion similar to the Taylor expansion of the function u_n, and we are able to tell exactly the order of the scheme by looking at the coefficients β_ℓ. The exact Taylor expansion is provided by:

$$u_{n+1} = \sum_{\ell=0}^{+\infty} \frac{\delta t^\ell}{\ell!} \partial_t^\ell u_n = u_n + \delta t \partial_t u_n + \frac{1}{2} \delta t^2 \partial_t^2 u_n + \frac{1}{6} \delta t^3 \partial_t^3 u_n + \dots \tag{4.6}$$

and the smallest $\ell - 1$ for which $\beta_\ell \neq 1/\ell!$ gives us the order of the scheme.

The interest of such schemes is that the coefficients α_ℓ are easily deduced from the β_ℓ. If the following relation

$$\langle F^i(u_n), F^j(u_n)\rangle_{L^2(\Omega)} = \begin{cases} 0 & \text{if} \quad i+j = 2\ell+1 \quad \text{for} \quad \ell \in \mathbb{N} \\ (-1)^{\ell-i}\|F^\ell(u_n)\|^2_{L^2} & \text{if} \quad i+j = 2\ell \quad \text{for} \quad \ell \in \mathbb{N} \end{cases} \tag{4.7}$$

is verified, which is the case for transport equation for instance, we have:

$$\|u_{n+1}\|^2_{L^2} = \|u_n\|^2_{L^2} + (\beta_1^2 - 2\beta_2)\delta t^2\|F(u_n)\|^2_{L^2} + (\beta_2^2 - 2\beta_1\beta_3 + 2\beta_4)\delta t^4\|F^2(u_n)\|^2_{L^2} \\ +(\beta_3^2 - 2\beta_2\beta_4 + 2\beta_1\beta_5 - 2\beta_6)\delta t^6\|F^3(u_n)\|^2_{L^2} + \dots$$

we put, as in (5.7), $S_m = \beta_m^2 - 2\beta_{m-1}\beta_{m+1} + 2\beta_{m-2}\beta_{m+2} + \dots$, so

$$\|u_{n+1}\|^2_{L^2} = \|u_n\|^2_{L^2} + S_1\delta t^2\|F(u_n)\|^2_{L^2} + S_2\delta t^4\|F^2(u_n)\|^2_{L^2} + S_3\delta t^6\|F^3(u_n)\|^2_{L^2} + \dots \tag{4.8}$$

Let F represent a hyperbolic operator with one derivative in x so that $\|F^r(u_n)\| \leq \frac{A_r}{\delta x^r}\|u_n\|$, and let $S_1 = \cdots = S_{r-1} = 0$ and $S_r > 0$. Then the von Neumann stability condition $\|u_{n+1}\|_{L^2} \leq (1 + C\delta t)\|u_n\|_{L^2}$ which corresponds to the exponential growth of the stability error $u_t \sim e^{Ct}$ for a given C, implies:

$$\frac{S_r A_r^2 \delta t^{2r}}{2\delta x^{2r}} \leq C\delta t \tag{4.9}$$

i.e.

$$\delta t \leq \left(\frac{2C}{S_r A_r^2}\right)^{1/(2r-1)} \delta x^{2r/(2r-1)} \tag{4.10}$$

For transport equation $F(u) = a\,\partial_x u$, $A_r = a^r$ and a CFL-like condition appears:

$$\delta t \leq \left(\frac{2C}{S_r}\right)^{1/(2r-1)} \left(\frac{\delta x}{a}\right)^{2r/(2r-1)} \tag{4.11}$$

This leads to the following schemes with determined order and stability condition:

- with $\beta_1 = 1$ and $\beta_\ell = 0$ for $\ell \geq 2$, this is the Euler explicit scheme:

  $$u_{n+1} = u_n + \delta t F(u_n) \tag{4.12}$$

  $\beta_2 \neq \frac{1}{2}$ so it is of order 1, and $S_1 = 1$ implies $\delta t \leq 2C\left(\frac{\delta x}{a}\right)^2$.

- with $\beta_1 = 1$, $\beta_2 = 1/2$ and $\beta_\ell = 0$ for $\ell \geq 3$, this is a second order Runge-Kutta scheme:

  $$u_{n+1} = u_n + \delta t F(u_n + \frac{1}{2}\delta t F(u_n)) \tag{4.13}$$

  $\beta_3 \neq \frac{1}{6}$ so it is of order 2, and $S_2 = 1/4$ implies $\delta t \leq 2\,C^{1/3}\left(\frac{\delta x}{a}\right)^{4/3}$.

- with $\beta_1 = 1$, $\beta_2 = 1/2$, $\beta_3 = 1/8$ and $\beta_\ell = 0$ for $\ell \geq 4$, it is an order two numerical scheme ($\beta_3 \neq 1/6$),

  $$\text{(scheme 3)} \quad u_{n+1} = u_n + \delta t F(u_n + \frac{1}{2}\delta t F(u_n + \frac{1}{4}\delta t F(u_n))) \tag{4.14}$$

  and as $S_1 = S_2 = 0$ and $S_3 = 1/64$, we have the stability condition

  $$\delta t \leq 2^{7/5}\,C^{1/5}\left(\frac{\delta x}{a}\right)^{6/5}. \tag{4.15}$$

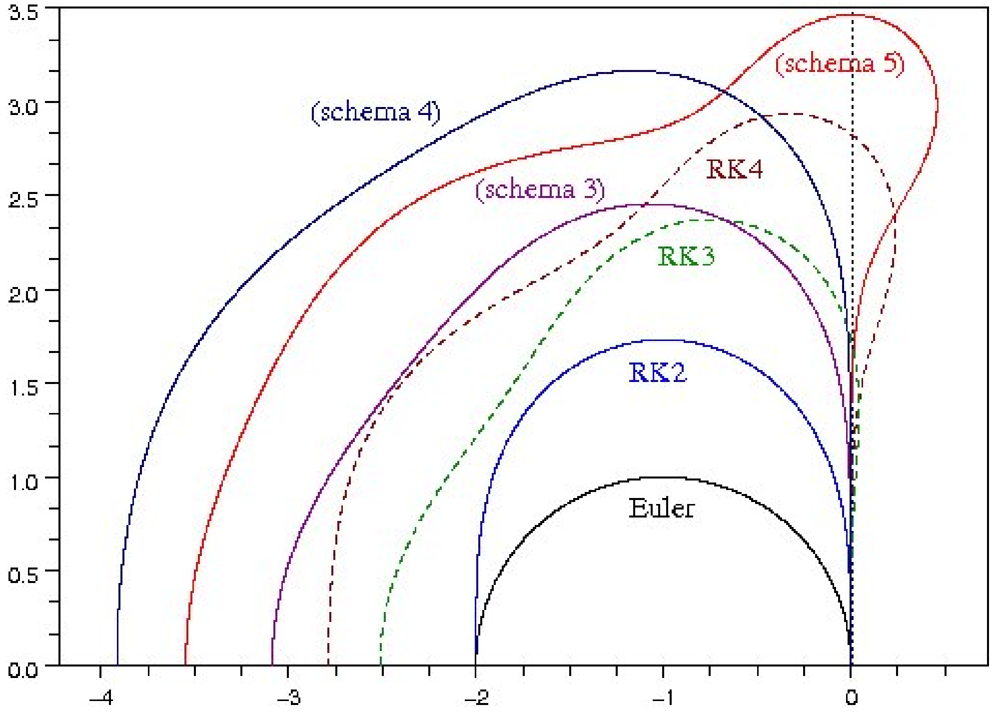

Figure 3: Von Neumann stability domains for schemes of Runge-Kutta type.

- the schemes verifying $\beta_\ell = 0$ for $\ell \geq 5$, and $S_1 = S_2 = S_3 = 0$ is given by $\beta_1 = 1$, $\beta_2 = 1/2$, $\beta_3 = \frac{2\pm\sqrt{2}}{4}$ and $\beta_4 = \frac{3\pm2\sqrt{2}}{8}$. If we choose the minus sign for β_3 and β_4, this means:

$$\text{(scheme 4)} \quad u_{n+1} = u_n + \delta t F(u_n + \frac{1}{2}\delta t F(u_n + \frac{2-\sqrt{2}}{2}\delta t F(u_n + \frac{2-\sqrt{2}}{4}\delta t F(u_n)))) \tag{4.16}$$

  It is a second order scheme and has the CFL-like stability condition

$$\delta t \leq \left(\frac{2C}{\beta_4^2}\right)^{1/7} \left(\frac{\delta x}{a}\right)^{8/7}. \tag{4.17}$$

- the scheme such that $\beta_\ell = 0$ for $\ell \geq 6$ and maximizing the number of S_ℓ equal to zero is given by $\beta_1 = 1$, $\beta_2 = 1/2$, $\beta_3 = 1/6$, $\beta_4 = 1/24$ and $\beta_5 = 1/144$. Hence it is written

$$\text{(scheme 5)} \quad u_{n+1} = u_n + \delta t F(u_n + \frac{\delta t}{2} F(u_n + \frac{\delta t}{3} F(u_n + \frac{\delta t}{4} F(u_n + \frac{\delta t}{6} F(u_n))))) \tag{4.18}$$

  As $S_5 = \beta_4^2 - 2\beta_3\beta_5 < 0$, we can not apply our stability criterion but a classical CFL condition $\delta t \leq C\frac{\delta x}{a}$. As $\beta_\ell = 1/\ell!$ until $\ell = 4$, this scheme is order 4.

In figure 4, the slopes of stability condition issued from numerical experiments confirm our predictions for these schemes.

5 Extension to some non-linear equations

We propose to extend these stability results to non-linear Navier-Stokes equations in four steps:

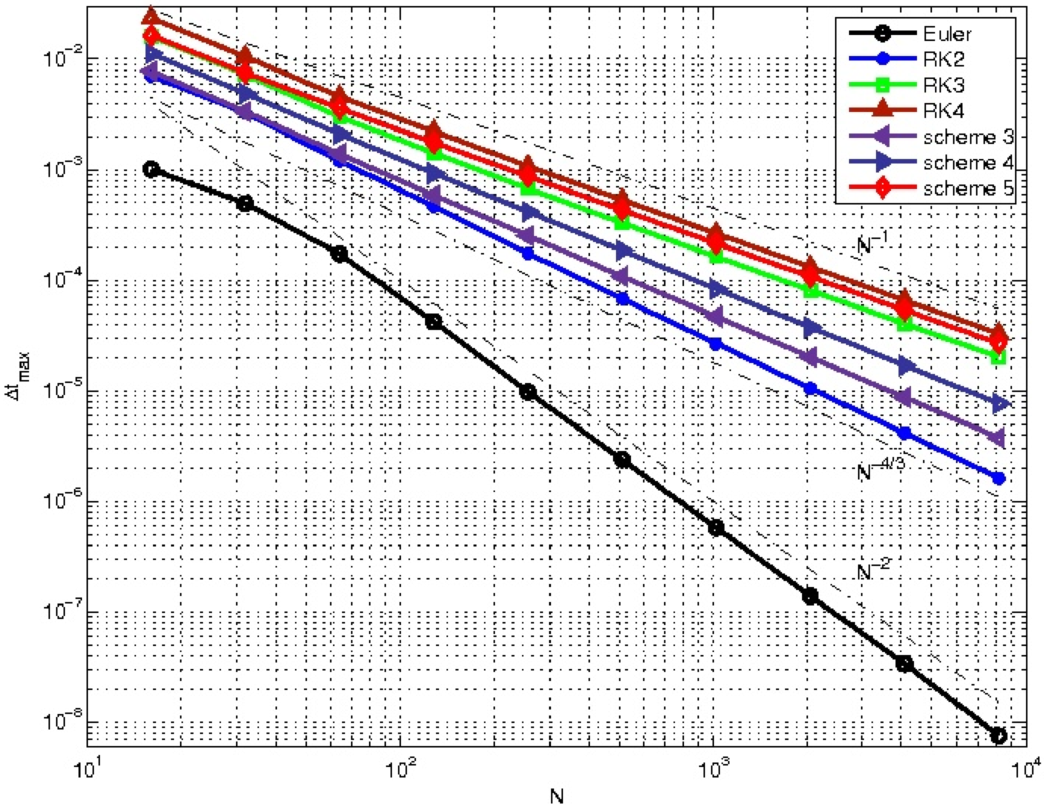

Figure 4: Stability conditions obtained experimentally with the 1-D Burgers equation (5.12) for schemes satisfying stability conditions of the type $\delta t \leq C\delta x^{2r/(2r-1)}$ for r an integer.

- First we consider the transport equation with non constant velocity on bounded domains. Hence we go out of the strict frame of von Neumann stability analysis.
- Then we study the most simple non-linear equation of transport type: the 1D Burgers equation, and show that the previous results are still valid under some smoothness condition of the solution. We also introduce the numerical experiment used to test our stability assumptions.
- Then we transpose our results to the incompressible Euler equations.
- And finally, we show that, when the viscosity plays a minor role in comparison with the transport –i.e. when the Reynolds number is large– the numerical schemes behave like in the previous cases. In addition, we show by a numerical experiment that boundaries do not interfere with the stability condition.

5.1 Transport by a non-constant velocity

We consider the transport of a scalar θ by a divergence-free velocity $\mathbf{u}$ on an open set $\Omega \subset \mathbb{R}^d$ with regular boundaries:

$$\partial_t\theta + \mathbf{u}(\mathbf{x}) \cdot \nabla\theta = 0, \text{ and } \operatorname{div}(\mathbf{u}) = 0 \quad \text{for } \mathbf{x} \in \Omega,\ t \in [0.T], \qquad \mathbf{u}(x) \cdot \mathbf{n} = 0 \quad \text{for } \mathbf{x} \in \partial\Omega \tag{5.1}$$

In order to generalize the stability analysis to this case, we need the following lemma (see [12], chapter IV, Lemma 2.1 or [6] for the proof, also used in [9]):

Lemma 5.1 *Let $\theta, \theta' : \Omega \to \mathbb{R}$, $\mathbf{u} : \Omega \to \mathbb{R}^d$ such that div($\mathbf{u}$)$= 0$ on Ω, and $\mathbf{u} \cdot \mathbf{n} = 0$ on $\partial\Omega$ then:*

$$\langle \theta, \mathbf{u} \cdot \nabla\theta' \rangle_{L^2(\Omega)} = -\langle \mathbf{u} \cdot \nabla\theta, \theta' \rangle_{L^2(\Omega)} \tag{5.2}$$

As a result, we also have:

$$\langle \theta, \mathbf{u} \cdot \nabla\theta \rangle_{L^2(\Omega)} = 0 \tag{5.3}$$

Let $F(\theta) = \mathbf{u} \cdot \nabla\theta$, or $F(\theta) = P_{\delta x}(\mathbf{u} \cdot \nabla\theta)$ if we take the space discretization into account and note $P_{\delta x}$ the orthogonal projector onto the space of discretization.

For the scheme (2.2), we find the following expression for θ_{n+1}:

$$\theta_{n+1} = \sum_{i=0}^{k} \beta_i \delta t^i F^i(\theta_n) \tag{5.4}$$

Starting from this expression and using the fact that according to lemma 5.2,

$$\langle F^i(\theta_n), F^j(\theta_n) \rangle_{L^2(\Omega)} = \begin{cases} 0 & \text{if} \quad i+j = 2\ell+1 \quad \text{for} \quad \ell \in \mathbb{N} \\ (-1)^{\ell-i} \|F^\ell(\theta_n)\|_{L^2}^2 & \text{if} \quad i+j = 2\ell \quad \text{for} \quad \ell \in \mathbb{N} \end{cases} \tag{5.5}$$

we compute the L^2 norm of θ_{n+1} as a function of the L^2 norm of θ_n:

$$\|\theta_{n+1}\|_{L^2}^2 = \sum_{\ell=0}^{k} S_\ell \, \delta t^{2\ell} \|F^\ell(\theta_n)\|_{L^2}^2 + o() \tag{5.6}$$

with

$$S_\ell = \sum_{j=-\min(\ell,k-\ell)}^{\min(\ell,k-\ell)} (-1)^j \beta_{\ell-j}\beta_{\ell+j} \tag{5.7}$$

For consistency needs of the numerical scheme, we must have $S_0 = 1$. If, on the other hand we suppose $S_1 = S_2 = \cdots = S_{r-1} = 0$ and $S_r > 0$, knowing that in the discretised space $V_{\delta x}$,

$$\|F^r(\theta_n)\|_{L^2} \leq \|\mathbf{u}_n\|_{L^\infty}^r \frac{\|\theta_n\|_{L^2}}{\delta x^r} \tag{5.8}$$

and knowing that for $x \geq -1$

$$\sqrt{1+x} \leq 1 + \frac{x}{2} \tag{5.9}$$

we derive:

$$\|\theta_{n+1}\|_{L^2} \leq \left(1 + \left(\frac{\delta t^{2r-1} S_r}{2\delta x^{2r}} \|\mathbf{u}_n\|_{L^\infty}^{2r} + o(1)\right) \delta t\right) \|\theta_n\|_{L^2} \tag{5.10}$$

where $o()$ gathers all the negligible terms.
Let us note $\|\mathbf{u}_n\|_{L^\infty} \leq A_0$, then the numerical scheme (2.2) is stable for small perturbations under the condition:

$$\delta t \leq C \delta x^{\frac{2r}{2r-1}} \tag{5.11}$$

Hence the results obtained in the von Neumann stability framework remain up to date in the case of the advection by a non-constant velocity on a bounded domain which is still linear but outside the von Neumann stability analysis framework.

5.2 The Burgers equation

In order to clarify the role of the non-linearity and validate our analysis under smoothness conditions on the solution, we will study the most simple non-linear case, the one-dimensional (as some inequalities are affected by the dimensionality, we introduce d sometimes) inviscid Burgers equation:

$$\partial_t u + u \partial_x u = 0 \quad \text{for} \quad (x,t) \in \mathbb{R} \times [0,T]. \tag{5.12}$$

We start from a discretization u_n of the solution u in time and in space. Then we consider a perturbed solution $u_n + \varepsilon_n$. Assuming the regularity of u and the consistency of the scheme, we are interested in the evolution of the perturbation ε_n for different explicit schemes in time.

Actually, the small error ε_n that we introduce corresponds to oscillations at the smallest scale in space $V_{\delta x}$. This stability error propagates and may increase at each time step. In what follows, we demonstrate that under some precise CFL-like conditions, the L^2 norm of this small error ε_n is amplified such that:

$$\|\varepsilon_{n+1}\|_{L^2} \leq (1 + C\delta t)\|\varepsilon_n\|_{L^2} \tag{5.13}$$

where C is a constant that neither depends on δx nor on δt.
Thus, after a time elapse T, the error increases at most exponentially as a function of the time:

$$\|\varepsilon_{t_0+T}\|_{L^2} \leq (1 + C\delta t)^{T/\delta t} \|\varepsilon_{t_0}\|_{L^2} \leq e^{CT} \|\varepsilon_{t_0}\|_{L^2} \tag{5.14}$$

As $\partial_t u = -u\partial_x u$, $\partial_t^\ell u = \sum_\alpha \lambda_\alpha u^{\alpha_1} (\partial_x u)^{\alpha_2} \ldots (\partial_x^{\ell-1} u)^{\alpha_{\ell-1}} + (-1)^\ell u^\ell \partial_x^\ell u$, so we remark that there is a kind of equivalence between the space regularity and the time regularity. At least, if $\partial_x^\ell u \in L^\infty$ then $\partial_t^\ell u \in L^\infty$. In the general case with the scheme (2.2), we have for $0 \leq \ell \leq s$,

$$u_{(\ell)} + \varepsilon_{(\ell)} = \sum_{i=0}^{\ell-1} a_{\ell i} \left(u_{(i)} + \varepsilon_{(i)}\right) + \delta t \sum_{i=0}^{\ell-1} b_{\ell i} \, F(u_{(i)} + \varepsilon_{(i)}) \tag{5.15}$$

and $u_{n+1} = u_{(s)}$, so

$$\varepsilon_{(\ell)} = \sum_{i=0}^{\ell-1} a_{\ell i}\, \varepsilon_{(i)} + \delta t \sum_{i=0}^{\ell-1} b_{\ell i}\, (F(u_{(i)} + \varepsilon_{(i)}) - F(u_{(i)})) \tag{5.16}$$

and $\varepsilon_{n+1} = \varepsilon_{(s)}$.

Theorem 5.1 *For $\delta t = o(\delta x)$, u s-times differentiable such that $\|\partial_x^s u\|_{L^\infty(\mathbb{R}\times[0,T])} < +\infty$, a stability error ε_{n+1} issued from an explicit scheme, small enough at the initial time: $\|\varepsilon_0\|_{L^2} = o(\delta x^{3/2})$ can be put under the form*

$$\varepsilon_{n+1} = \varepsilon_n + \sum_{i=1}^{s} \beta_i \delta t^i u_n^i \partial_x^i \varepsilon_n + \delta t \varepsilon_n \partial_x u_n + R_n \tag{5.17}$$

with $\|R_n\|_{L^2} = o(\delta t \|\varepsilon_n\|_{L^2})$. The coefficients (β_i) are obtained similarly as those in (3.3).

proof: All the terms we have to deal with are projections in the space discretization $V(\delta x)$. In order to lighten the notation, we omit this projection that we assume orthogonal.
We prove that $\varepsilon_{(\ell)}$ can be put under the form (5.17) by recurrence on $\ell = 0 \ldots s$.
As $\varepsilon_{(0)} = \varepsilon_n$, the assertion is true for $\ell = 0$.
Let us assume the assertion true for i from 0 to $\ell - 1$:

$$\varepsilon_{(i)} = \varepsilon_n + \sum_{j=1}^{i} \beta_{(i)j} \delta t^j u_n^j \partial_x^j \varepsilon_n + \alpha_{(i)} \delta t \varepsilon_n \partial_x u_n + R_{(i)} \tag{5.18}$$

with $\|R_{(i)}\|_{L^2} = o(\delta t \|\varepsilon_n\|_{L^2})$. The coefficients $(\beta_{(i)j})$ correspond to the partial step i of the Runge-Kutta scheme distant by $\alpha_{(i)}\delta t$ from the time $i\delta t$. Remark that $\alpha = \alpha_{(s)} = 1$. Then, given that $\sum_{i=0}^{\ell-1} a_{\ell i} = 1$,

$$\begin{aligned}
\varepsilon_{(\ell)} &= \sum_{i=0}^{\ell-1} a_{\ell i}\, \varepsilon_{(i)} + \delta t \sum_{i=0}^{\ell-1} b_{\ell i}\, (F(u_{(i)} + \varepsilon_{(i)}) - F(u_{(i)})) \\
&= \varepsilon_n + \sum_{i=0}^{\ell-1} a_{\ell i} \left(\sum_{j=1}^{i} \beta_{(i)j} \delta t^j u_n^j \partial_x^j \varepsilon_n + \alpha_{(i)} \delta t \varepsilon_n \partial_x u_n + R_{(i)} \right) \\
&\quad + \delta t \sum_{i=0}^{\ell-1} b_{\ell i}\, \left(u_{(i)} \partial_x \varepsilon_{(i)} + \varepsilon_{(i)} \partial_x u_{(i)} + \varepsilon_{(i)} \partial_x \varepsilon_{(i)} \right)
\end{aligned} \tag{5.19}$$

knowing that

$$\partial_x \varepsilon_{(i)} = \partial_x \varepsilon_n + \sum_{j=1}^{i} \beta_{(i)j} \delta t^j \left(\partial_x (u_n^j) \partial_x^j \varepsilon_n + u_n^j \partial_x^{j+1} \varepsilon_n \right) + \alpha_{(i)} \delta t \left(\partial_x \varepsilon_n \partial_x u_n + \varepsilon_n \partial_x^2 u_n \right) + \partial_x R_{(i)}. \tag{5.20}$$

Hence

$$\begin{aligned}
R_{(\ell)} &= \sum_{i=0}^{\ell-1} a_{\ell i}\, R_{(i)} + \delta t \sum_{i=0}^{\ell-1} b_{\ell i} \left(u_{(i)} \left(\sum_{j=1}^{i} \beta_{(i)j} \delta t^j \partial_x (u_n^j) \partial_x^j \varepsilon_n + \delta t \left(\partial_x \varepsilon_n \partial_x u_n + \varepsilon_n \partial_x^2 u_n \right) + \partial_x R_{(\ell)} \right) \right. \\
&\quad \left. + \varepsilon_{(i)} \partial_x \varepsilon_{(i)} + (\varepsilon_{(i)} \partial_x u_{(i)} - \varepsilon_n \partial_x u_n) + (u_{(i)} - u_n) \sum_{j=1}^{i} \beta_{(i)j} \delta t^j u_n^j \partial_x^{j+1} \varepsilon_n \right)
\end{aligned} \tag{5.21}$$

Now, we need to show that these terms are $o(\delta t\|\varepsilon_n\|_{L^2})$. Thanks to assumption (5.18), $\varepsilon_{(i)} = (1+o(1))\varepsilon_n$ in the sense $\varepsilon_{(i)} = \varepsilon_n + \eta_{(i)}$ with $\|\eta_{(i)}\|_{L^2} = o(\|\varepsilon_n\|_{L^2})$ (the stability condition being $\|\varepsilon_{(i)}\|_{L^2} = (1+O(\delta t))\|\varepsilon_n\|_{L^2}$). As we assumed $\|\varepsilon_n\|_{L^2} = o(\delta x^{3/2})$, then (with $d=1$ in our case),

$$\|\varepsilon_n\|_{L^\infty} \leq \frac{\|\varepsilon_n\|_{L^2}}{\delta x^{d/2}} = o(\delta x) \tag{5.22}$$

As a result, the cross term $\delta t\varepsilon_{(i)}\partial_x\varepsilon_{(i)}$ satisfies

$$\|\delta t\varepsilon_{(i)}\partial_x\varepsilon_{(i)}\|_{L^2} \leq \frac{\delta t}{\delta x}\|\varepsilon_{(i)}\|_{L^\infty}\|\varepsilon_{(i)}\|_{L^2} = o(\delta t\|\varepsilon_n\|_{L^2}) \tag{5.23}$$

As for $i \leq s-1$,

$$u_{(i)} = u_n + \delta t B_{(i)}(u_n, \partial_x u_n, \ldots, \partial_x^i u_n, \delta t) \tag{5.24}$$

with B a polynomial, $\|B\|_{L^\infty}$ is bounded, as well as $\|\partial_x B\|_{L^\infty}$ so $\|u_{(i)} - u_n\|_{L^\infty}$=o(1) and $\|\partial_x u_{(i)} - \partial_x u_n\|_{L^\infty}$=o(1). It allows us to replace $u_{(i)}$ by u_n in the expansion (5.19), the difference going into $R_{(\ell)}$, see (5.21).

Hence, using the fact that $\varepsilon_{(i)}, R_{(i)} \in V(\delta x)$ the discretization space, $\|\partial_x^j\varepsilon_{(i)}\|_{L^2} \leq \frac{\|\varepsilon_{(i)}\|_{L^2}}{\delta x^j}$ and the same for $R_{(i)}$. Let r be an element of the sum $R_{(\ell)}$, then it satisfies:

$$\|r\| \leq \frac{\delta t^p}{\delta x^q}\tau(\|u_n\|_{L^\infty}, \|\partial_x u_n\|_{L^\infty}, \ldots, \|\partial_x^\ell u_n\|_{L^\infty})\|\varepsilon_n\|_{L^2} \tag{5.25}$$

with τ a polynomial, and $p \geq q+1$.

Given the fact that $\delta t = o(\delta x)$, we obtain that $\|R_{(\ell)}\|_{L^2} = o(\delta t\|\varepsilon_n\|_{L^2})$. Using the recurrence, we obtain the result for $\ell = s$ i.e. for ε_{n+1}.

Actually, taking into account the orthogonality of $\varepsilon_n\partial_x\varepsilon_n$ with ε_n, we can relax one of the assumptions i.e. it is sufficient to have $\|\varepsilon_0\|_{L^2} = o(\delta x^{1/2+d/2})$, and with the cancellations, it is even only necessary that $\|\varepsilon_0\|_{L^2} = o(\delta x^{d/2})$, with $d=1$ in our case.

□

Thanks to theorem 5.1, we are able to write:

$$\|\varepsilon_{n+1}\|_{L^2} \leq \|\varepsilon_n + \sum_{i=1}^{s}\beta_i\delta t^i u_n^i\partial_x^i\varepsilon_n\|_{L^2} + \delta t\|\varepsilon_n\partial_x u_n\|_{L^2} + o(\delta t\|\varepsilon_n\|_{L^2}) \tag{5.26}$$

On the other hand we have $\|\varepsilon_n\partial_x u_n\|_{L^2} \leq \|\partial_x u\|_{L^\infty}\|\varepsilon_n\|_{L^2}$ and

$$\|\varepsilon_n + \sum_{i=1}^{s}\beta_i\delta t^i u_n^i\partial_x^i\varepsilon_n\|_{L^2}^2 = \sum_{\ell=0}^{2s} S_\ell\delta t^\ell\|u_n^\ell\partial_x^\ell\varepsilon_n\|_{L^2}^2 + o(\delta t\|\varepsilon_n\|_{L^2}^2) \tag{5.27}$$

with S_i given by (3.5), since for $i, j \leq s$,

$$\langle\delta t^i u_n^i\partial_x^i\varepsilon_n, \delta t^j u_n^j\partial_x^j\varepsilon_n\rangle_{L^2} = \begin{cases} o(\delta t\|\varepsilon_n\|_{L^2}^2) & \text{if} \quad i+j = 2\ell+1 \\ (-1)^{\ell-i}\delta t^{2\ell}\|u_n^\ell\partial_x^\ell\varepsilon_n\|_{L^2}^2 + o(\delta t\|\varepsilon_n\|_{L^2}^2) & \text{if} \quad i+j = 2\ell \end{cases} \tag{5.28}$$

Then, as $S_0 = 1$, and $\|u_n^\ell\partial_x^\ell\varepsilon_n\|_{L^2} \leq \|u_n\|_{L^\infty}^\ell\frac{\|\varepsilon_n\|_{L^2}}{\delta x^\ell}$,

$$\|\varepsilon_n + \sum_{i=1}^{s}\beta_i\delta t^i u_n^i\partial_x^i\varepsilon_n\|_{L^2}^2 \leq \sum_{\ell=0}^{2s} S_\ell\left(\frac{\delta t}{\delta x}\right)^{2\ell}\|u\|_{L^\infty}^{2\ell}\|\varepsilon_n\|_{L^2}^2 + o(\delta t\|\varepsilon_n\|_{L^2}^2) \tag{5.29}$$

so

$$\|\varepsilon_n + \sum_{i=1}^{s} \beta_i \delta t^i u_n^i \partial_x^i \varepsilon_n\|_{L^2} \leq \left(1 + \frac{1}{2}\sum_{\ell=1}^{2s} S_\ell \left(\frac{\delta t}{\delta x}\right)^{2\ell} \|u\|_{L^\infty}^{2\ell} + o(\delta t)\right) \|\varepsilon_n\|_{L^2} \tag{5.30}$$

and finally

$$\|\varepsilon_{n+1}\|_{L^2} \leq \left(1 + \frac{1}{2}\sum_{\ell=1}^{2s} S_\ell \left(\frac{\delta t}{\delta x}\right)^{2\ell} \|u\|_{L^\infty}^{2\ell} + \delta t \|\partial_x u\|_{L^\infty} + o(\delta t)\right) \|\varepsilon_n\|_{L^2} \tag{5.31}$$

Let r be the first power in the sum where $S_r \neq 0$, and let us assume that $S_r > 0$. Then, the stability condition $\|\varepsilon_{n+1}\|_{L^2} \leq (1 + C\delta t) \|\varepsilon_n\|_{L^2}$ is reduced to

$$\frac{1}{2} S_r \frac{\delta t^{2r-1}}{\delta x^{2r}} \|u\|_{L^\infty}^{2r} \leq (C - \|\partial_x u\|_{L^\infty}) \tag{5.32}$$

i.e.

$$\delta t \leq \left(\frac{2(C - \|\partial_x u\|_{L^\infty})}{S_r}\right)^{\frac{1}{2r-1}} \left(\frac{\delta x}{\|u\|_{L^\infty}}\right)^{\frac{2r}{2r-1}}. \tag{5.33}$$

We recognize same power law as obtained in the linear case (4.11).

Numerical experiment

We now proceed to a numerical experiment with the inviscid Burgers equation

$$\partial_t u + u \partial_x u = 0 \quad \text{for} \quad (x, t) \in \mathbb{T} \times [0, T]. \tag{5.34}$$

Here we show numerical evidence that stability conditions (3.16), (3.18), (3.25) and (3.27) hold for this problem (replacing a by $\|u\|_{L_\infty}$).

Let us solve equation (5.34) numerically using a Fourier pseudo-spectral method [2]. Conservative formulation of the quadratic term is used, and the scheme is de-aliased by truncation. Time integration methods include the explicit Euler scheme, second to fourth order Runge–Kutta schemes, and second to fifth order Adams–Bashforth schemes, with the exact solution being used for startup.

The initial condition for the numerical experiments is $u_0(x) = 10 - 0.1 \sin(\pi x)$, hence the periodic domain in x is $\Omega = [-1, 1]$. For $t < t_{max} = 10/\pi$ the equation admits a smooth exact solution $u(x,t) = u_0(a)$, where $a = a(x,t) : a - x + u_0(a)t = 0$. However, the numerical solution is only sought for $t \in [0, 1]$, as to require a reasonable number of Fourier modes and to avoid Gibbs oscillations which would complicate the use of stability criterion. The latter is based on the total variation norm, we call the numerical solution $v(x,t)$ stable when $||v(x,t)||_{TV} < K||u_0(x)||_{TV}$, and we set $K = 5$.

The $\delta t_{\max}$ we compute, has very little dependence on the divergence criterion. actually, below this limit (97%), the numerical solution shows no spurious oscillations, while above it (103%), these oscillations create some kind of explosion destroying the profile of the solution completely, see figure 5.

The computations are performed for different number of grid points, $N = 2^4 ... 2^{13}$. For each N we use dichotomy to find the stability limit δt_{max}. The results are represented as $\delta t_{max}(N)$ curves in Fig. 6. They evidence the theoretically predicted power law $\Delta t_{max} = CN^\alpha$ when the number of grid points is sufficiently large, $N > 64$. The explicit Euler

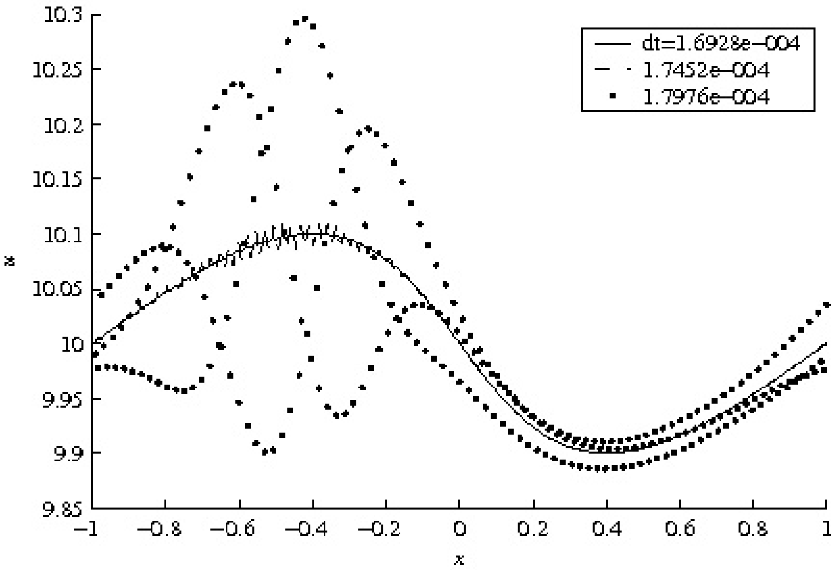

Figure 5: Numerical solution obtained at time T for three different time steps: $0.97\,\delta t_{\max}$, $\delta t_{\max}$ and $1.03\,\delta t_{\max}$.

scheme displays $\alpha = -2$ slope. The two curves corresponding to the second-order schemes asymptotically both have $-4/3$ slope, but the constant C is $2^{1/3}$ times larger for the Runge–Kutta scheme.

When the order is increasing to 3 and 4, Runge–Kutta schemes become more stable: the slope equals -1, and the constant is increasing. For the third-, fourth- and fifth-order Adams–Bashforth schemes the slope equals $\alpha = -1$ as well, but the constant C diminishes with the increasing order. Hence, the fourth-order Runge–Kutta scheme allows 6.575 times larger steps than the Adams–Bashforth scheme of the same order. The latter result is, though, classical, and it can be deduced from linear stability regions of the two schemes (see figure 1 or *e.g.*, [2]).

5.3 Incompressible Euler equation

The Euler equations modelise incompressible fluid flows with no viscous term:

$$\frac{\partial \mathbf{u}}{\partial t} + (\mathbf{u} \cdot \nabla)\mathbf{u} - \nabla p = 0, \qquad \operatorname{div} \mathbf{u} = 0 \tag{5.35}$$

The use of the Leray projector $\mathbb{P}$ which is the L^2-orthogonal projector on the divergence-free space, allows us to remove the pressure term:

$$\frac{\partial \mathbf{u}}{\partial t} + \mathbb{P}\left[(\mathbf{u} \cdot \nabla)\mathbf{u}\right] = 0 \tag{5.36}$$

The following stability study somehow works as a synthesis of the previous two sections 5.1 and 5.2. An important property is then the skewness property of the transport term, which is utilized for the stability of the incompressible Navier-Stokes equations in [9].

Lemma 5.2 *Let* $\mathbf{u}, \mathbf{v}, \mathbf{w} \in H^1(\Omega)^d$*,* $H^1(\Omega)$ *denoting the Sobolev space on the open set* $\Omega \subset \mathbb{R}^d$*, be such that* $(\mathbf{u} \cdot \nabla)\mathbf{v}, (\mathbf{u} \cdot \nabla)\mathbf{w} \in L^2$*. If* $\mathbf{u} \in \boldsymbol{H}_{\mathrm{div},0}(\Omega) = \{\mathbf{f} \in (L^2(\Omega)))^d,\ \operatorname{div} \mathbf{f} =$

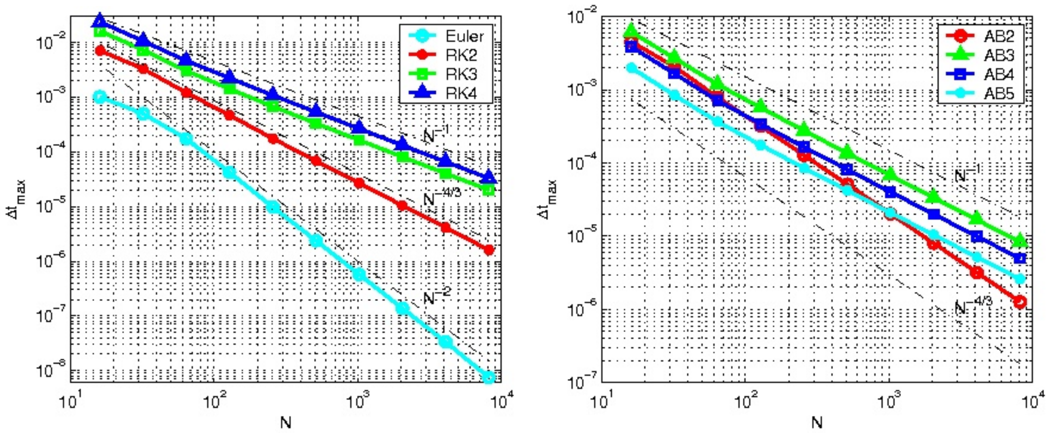

Figure 6: Stability condition for Runge–Kutta schemes (left) and Adams–Bashforth schemes (right).

$0\}$, *then*

$$\langle \mathbf{v}, (\mathbf{u}\cdot\nabla)\mathbf{w}\rangle_{L^2(\Omega)} = -\langle (\mathbf{u}\cdot\nabla)\mathbf{v}, \mathbf{w}\rangle_{L^2(\Omega)} \tag{5.37}$$

Corollary 5.1 *With the same assumptions as in lemma 5.2,*

$$\langle \mathbf{v}, (\mathbf{u}\cdot\nabla)\mathbf{v}\rangle_{L^2(\Omega)} = \int_{\mathbf{x}\in\Omega} \mathbf{v}\cdot(\mathbf{u}\cdot\nabla)\mathbf{v}\, d\mathbf{x} = 0 \tag{5.38}$$

In the scheme (2.2), we denote by $\varepsilon_{(\ell)}$ the stability error at level ℓ. Then, under the condition $\delta t = o(\delta x)$ and for ε_n small enough, most of the terms appearing in the expression of $\varepsilon_{(\ell)}$ become negligible compared with:

- the terms $\delta t^i\, F^i(\varepsilon_n)$ where $F(\varepsilon_n) = \mathbb{P}[(\mathbf{u}_n\cdot\nabla)\varepsilon_n]$ and $F^i = F\circ F\circ\cdots\circ F$, i times.
- the term $\delta t\, \mathbb{P}[(\varepsilon_n\cdot\nabla)\mathbf{u}_n]$,

Then most of the arguments used in section 5.2 can be reused with even more accuracy since we have the orthogonality relation (4.7) which stands instead of (5.28). This leads to the following result:

Theorem 5.2 *For a solution u of the Euler incompressible equation (5.35), s-times differentiable such that $\|\partial_x^s u\|_{L^\infty(\mathbb{R}\times[0,T])} < +\infty$, the stability condition associated to an error ε_{n+1} issued from an explicit scheme, small enough at the initial time: $\|\varepsilon_0\|_{L^2} = o(\delta x^{d/2})$, satisfies*

$$\delta t \le \left(\frac{2C}{S_r}\right)^{1/(2r-1)} \left(\frac{\delta x}{\|u\|_{L^\infty}}\right)^{\frac{2r}{2r-1}} \tag{5.39}$$

with δt the time step and δx the space step, and r obtained as in (5.7) and (5.10).

5.4 Navier-Stokes equations with a high Reynolds number

The incompressible Navier-Stokes equations are written:

$$\begin{cases} \partial_t\mathbf{u} + \mathbf{u}\cdot\nabla\mathbf{u} - \nu\Delta\mathbf{u} + \nabla p = 0, & \\ \mathrm{div}\mathbf{u} = 0, & x\in\mathbb{R}^d,\ t\in[0,T] \\ \mathbf{u}(0,x) = \mathbf{u}_0(x) & \end{cases} \tag{5.40}$$

Using the Leray projector $\mathbb{P}$ –the orthogonal projector on divergence-free vector fields– we reduce the equation to:

$$\partial_t \mathbf{u} + \mathbb{P}\left[\mathbf{u} \cdot \nabla \mathbf{u}\right] - \nu \Delta \mathbf{u} = 0 \tag{5.41}$$

We performed numerical experiments with two second order schemes that are widely used for the solution of this equation:

- a Runge-Kutta scheme with a mid-point $\mathbf{u}_{n+1/2}$

$$\left(Id - \nu \frac{\delta t}{2} \Delta\right) \mathbf{u}_{n+1/2} = \mathbf{u}_n - \frac{\delta t}{2} \mathbb{P}\left[(\mathbf{u}_n \cdot \nabla)\mathbf{u}_n\right] \tag{5.42}$$

  then $\mathbf{u}_{n+1}$ is given by:

$$\left(Id - \nu \frac{\delta t}{2} \Delta\right) \mathbf{u}_{n+1} = \mathbf{u}_n + \delta t \left(\frac{\nu}{2} \Delta \mathbf{u}_n - \mathbb{P}\left[(\mathbf{u}_{n+1/2} \cdot \nabla)\mathbf{u}_{n+1/2}\right]\right) \tag{5.43}$$

- a second order Adams-Bashforth scheme.
  With Fourier transform, the heat kernel $\partial_t \mathbf{u} = \nu \Delta \mathbf{u}$ integrates exactly by putting:

$$\widehat{\mathbf{v}}(\xi, t) = e^{\nu \xi^2 t} \widehat{\mathbf{u}}(\xi, t) \tag{5.44}$$

  Then we solve:

$$\partial_t \mathbf{v} + e^{-\nu t \Delta} \mathbb{P}\left[(e^{-\nu t \Delta} \mathbf{v} \cdot \nabla) e^{-\nu t \Delta} \mathbf{v}\right] = 0. \tag{5.45}$$

  By denoting $F(\mathbf{v}, t) = e^{-\nu t \Delta} \mathbb{P}\left[(e^{-\nu t \Delta} \mathbf{v} \cdot \nabla) e^{-\nu t \Delta} \mathbf{v}\right]$ and discretizing (5.45) in time, we obtain

$$\mathbf{v}_{n+1} = \mathbf{v}_n - \frac{3}{2} \delta t\, F(\mathbf{v}_n, n\delta t) + \frac{1}{2} \delta t\, F(\mathbf{v}_{n-1}, (n-1)\delta t) \tag{5.46}$$

When the Reynolds number $Re = \frac{\|u\| L}{\nu}$ is sufficiently large, the contribution of the heat kernel to the stability vanishes, and we observe the same instability effects as for incompressible Euler equation, see figure 7.

Numerical experiments

Two-dimensional Navier–Stokes equations

We consider the two-dimensional Navier–Stokes equations in the vorticity–streamfunction formulation,

$$\partial_t \omega + \mathbf{u} \cdot \nabla \omega - \nu \nabla^2 \omega = 0, \tag{5.47}$$

where $\omega = \nabla \times \mathbf{u}$ denotes the vorticity, which is a scalar field. The velocity is determined as a sum $\mathbf{u} = \nabla^{\perp} \Psi + \mathbf{U}_{\infty}$, with $\mathbf{U}_{\infty}$ being the free-stream velocity and Ψ being the stream function, satisfying

$$\nabla^2 \Psi = \omega, \tag{5.48}$$

where $\nabla^{\perp} \Psi = (-\partial_y \Psi, \partial_x \Psi)$ stands for orthogonal gradient of the stream function. The parameter ν is the kinematic viscosity.

The analysis in Section 3 can be applied to (5.47)-(5.48) and, when ν is sufficiently small, we can expect same stability condition as for the Euler equations.

This conjecture is confirmed with numerical experiments. We solve (5.47)-(5.48) using a pseudo-spectral method with dealiasing (see [11] for details of the model). The flow is

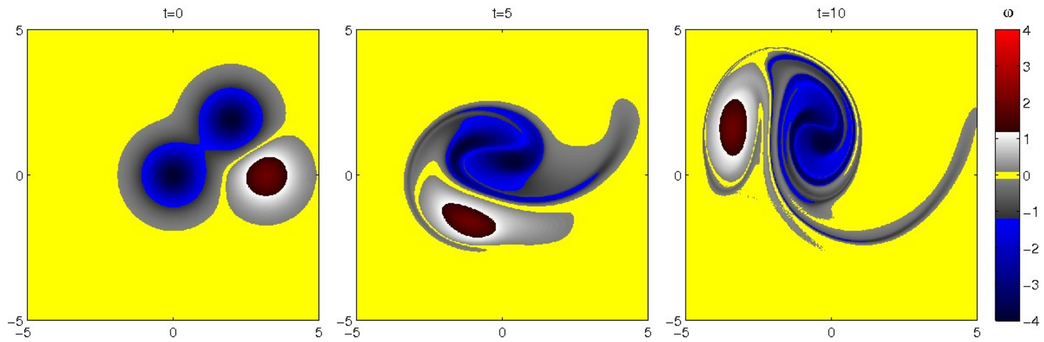

Figure 7: Time evolution of the vorticity.

in a square domain of size $L^2 = 10^2$, and conditions at the boundaries are periodic. As an initial condition we take three Gaussian vortices,

$$\omega_0 = -4e^{-(x^2+y^2)} - 4e^{-((x-1.98)^2+(y-1.9)^2)} + 2e^{-((x-3.16)^2+y^2)}. \tag{5.49}$$

The second order Adams–Bashforth scheme is used to advance the vorticity in time up to $t_{max} = 10$. Even in the limiting case $\nu = 0$ corresponding to the Euler equation, the solution apparently remains smooth within this time interval. This is seen in Fig. 7, which represents the vorticity field at three subsequent time instants.

For three different values of viscosity, $\nu = 10^{-2}$, $\nu = 10^{-3}$ and $\nu = 0$, we vary the spatial resolution N^2 from 64^2 to 2048^2, and determine the largest possible time step for a stable solution, δt_{max}. Total variation norm of the stream function is used as a stability criterion.

The results are summarized in Fig. 8. When $\nu = 0$ one can see that the largest possible time step δt_{max} is varying with the spatial resolution as $N^{-4/3}$, in agreement with the prediction in Section 3. When ν is not zero, the 4/3 slope is only observed when N is sufficiently small, and δt_{max} becomes constant at large N. This phenomenon was explained by [17].

Dipole/wall interaction

Now we test the impact of boundaries on the stability condition. In part 5.3, we predicted that it should have no effect. To simulate the presence of boundaries, we used a penalization method [1]. As initial condition for the vorticity, we take two Gaussian functions $A\,\pi\, e^{-4\,\pi^4\,((x-x_0)^2+(y-y_0)^2)}$ located at $(x_0, y_0) = (\frac{1}{2}, \frac{3}{8})$ and $(x_0, y_0) = (\frac{1}{2}, \frac{5}{8})$ with amplitudes $A = -2$ and $A = 2$ on a square $[0,1]^2$, with boundaries at $x \leq 1/16$ and $x \geq 15/16$ and periodic boundary conditions in the vertical direction. We also chose $\nu = 5e-5$.

Then the numerical solution evolves as illustrated in figure 9. Figure 10 displays the maximal time step as a function of the number of spatial grid points. Time discretization is Adams Bashforth 2 (5.46). The numerical tests are performed for three different values of the viscosity, $\nu = 0$, $\nu = 10^{-6}$ and $\nu = 10^{-7}$, and also for different values of the penalization parameter η, which is either fixed to a constant value or varies in proportion with δt. We should remind that the solution of the penalized Navier-Stokes equations converges in the limit $\eta \to 0$ to the solution of Navier-Stokes equations with the no-slip

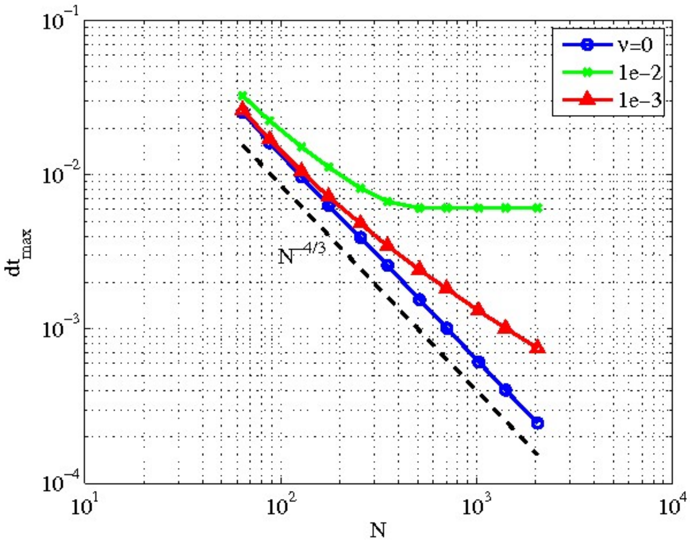

Figure 8: Largest possible time step in the numerical simulation of the flow induced by three vortices in a periodic domain.

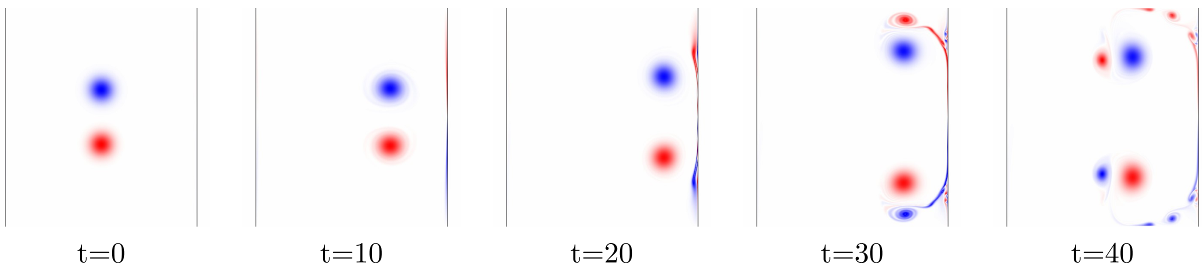

Figure 9: Dipole/wall interaction experiment in 512^2 resolution.

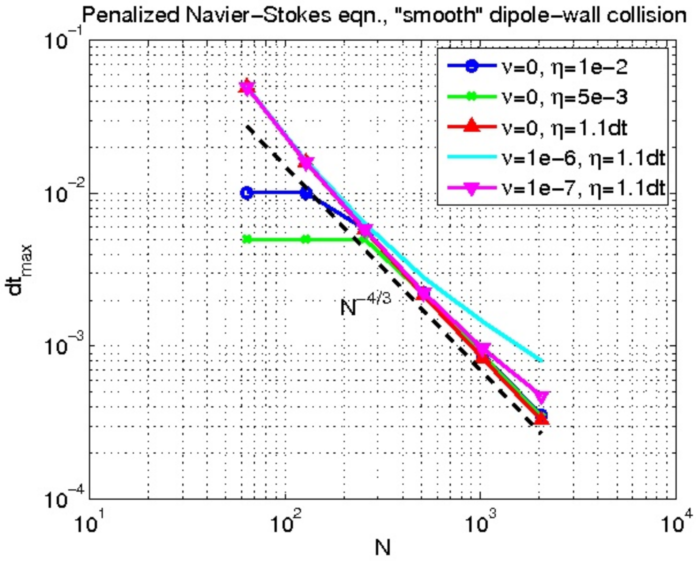

Figure 10: Stability dependence for the maximum time step $\delta t_{\max}$ to the space step δx in the dipole/wall interaction experiment (see fig 9).

boundary conditions [1]. All the curves in figure 10 exhibit the $N^{-4/3}$ slope in the range where convection is dominant over the viscous diffusion, as it was already observed in the previous example without boundaries.

The instabilities occur similarly to the previously studied case, which is the Burgers equation (see figure 5). The highest mode undergoes an excitation along the stream direction which drives to the numerical divergence, see figure 11.

5.5 Scalar conservation laws

Scalar conservation laws group equations of the type

$$\partial_t u + \sum_{i=1}^{d} \partial_{x_i} f_i(u) = 0 \quad \text{for} \quad (\mathbf{x}, t) \in \mathbb{R}^d \times [0, T] \tag{5.50}$$

$$u(0, \mathbf{x}) = u_0(\mathbf{x}) \quad \text{for} \quad \mathbf{x} \in \mathbb{R}^d \tag{5.51}$$

with $f_i : \mathbb{R} \to \mathbb{R}$ differentiable functions and $u : \mathbb{R}^d \to \mathbb{R}$ the scalar unknown function.
A stability analysis of the solution of these equations in the frame of Discontinuous Galerkin Runge-Kutta formulation was presented in [18] for order one and two, with the correct $\delta t \leq C\delta x^{4/3}$ CFL-like condition, but as the byproduct of a long and laborious process. This work was the continuation of [4] where the authors observed that first and second order Runge-Kutta methods are unstable under any linear CFL conditions when the space discretization is sufficiently accurate and so does not dissipate too much. In this paragraph, we link their result to our analysis and refine the stability criteria. Actually we have the following result:

Theorem 5.3 *Let us apply the numerical scheme (2.2) to solve the equation (5.50). If $f \in C^{p+1}$ and $u \in C^p$ i.e. $f^{(p+1)}, u^{(p)} \in L^\infty$, then similarly to equation (4.8) if $S_1 =$*

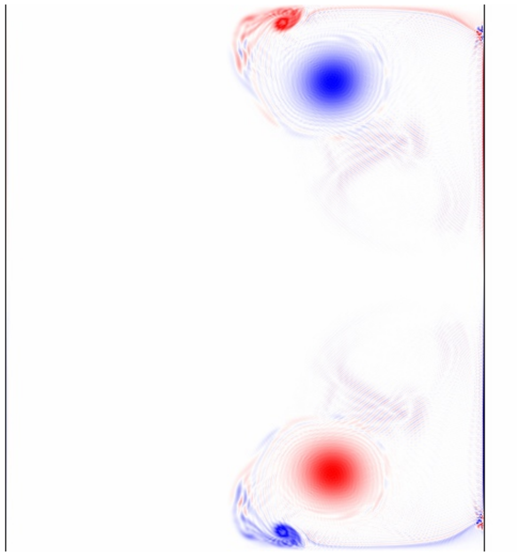

Figure 11: Instance of a high mode excitation in the dipole/wall experiment with Adams Bashforth order two scheme with 512^2 points.

$\cdots = S_{r-1} = 0$ *and* $S_r > 0$*, given a constant* C *limiting the growth of the stability error by* $\varepsilon_T \leq e^{CT}\varepsilon_0$*, the numerical scheme is conditionally stable under the CFL-like condition:*

$$\delta t \leq \left(\frac{2C}{S_r}\right)^{1/(2r-1)} \left(\frac{\delta x}{\sum_{i=1}^{d} \|f_i'(u)\|_{L^\infty}}\right)^{\frac{2r}{2r-1}}. \tag{5.52}$$

proof: The proof is more or less the same as for the Burgers case *cf* part 5.2, using the following facts:

- $f_i(u_n + \varepsilon_n) = f_i(u_n) + f_i'(u_n)\varepsilon_n + o(\varepsilon_n)$,
- $u_{(\ell)} - u_n = o(1)$,
- $\partial_{x_i}\left(f_i'(u_n)\varepsilon\right) \sim f_i'(u_n)\partial_{x_i}\varepsilon$ for stability analysis, and
- for all functions η and ε,

$$\left\langle \eta, \sum_{i=1}^{d}\sum_{j=1}^{d} \partial_{x_i}\left(f_i'(u_n)f_j'(u_n)\partial_{x_j}\varepsilon\right)\right\rangle = -\left\langle \sum_{i=1}^{d} f_i'(u_n)\partial_{x_i}\eta, \sum_{i=1}^{d} f_i'(u_n)\partial_{x_i}\varepsilon\right\rangle \tag{5.53}$$

  allowing equalities of the type (4.7)

Finally, we obtain:

$$\|\varepsilon_{n+1}\|_{L^2}^2 = (1 + 2C_1\delta t + o(\delta t))\|\varepsilon_n\|_{L^2}^2 + S_r\,\delta t^{2r}\left\|\sum_{i\in[1,d]^r}\left(\prod_{s=1}^{r} f_{i_s}'(u_n)\right)\left(\prod_{s=1}^{r}\partial_{x_{i_s}}\right)\varepsilon_n\right\|_{L^2}^2 \tag{5.54}$$

Then, knowing that for $\varepsilon_n \in V(\delta x)$,

$$\begin{aligned}\left\| \sum_{i\in[1,d]^r} \left(\prod_{s=1}^{r} f'_{i_s}(u_n)\right)\left(\prod_{s=1}^{r} \partial_{x_{i_s}}\right)\varepsilon_n \right\|_{L^2}^2 &\leq \left(\sum_{i\in[1,d]^r} \left(\prod_{s=1}^{r} \|f'_{i_s}(u_n)\|_{L^\infty}\right) \frac{\|\varepsilon_n\|_{L^2}}{\delta x^r} \right)^2 \\ &\leq \left(\left(\sum_{i\in[1,d]} \|f'_i(u_n)\|_{L^\infty} \right)^r \frac{\|\varepsilon_n\|_{L^2}}{\delta x^r} \right)^2, \end{aligned} \tag{5.55}$$

and neglecting the constant C_1, the von Neumann stability criteria

$$\|\varepsilon_{n+1}\|_{L^2}^2 \leq (1 + 2C\delta t + o(\delta t))\|\varepsilon_n\|_{L^2}^2 \tag{5.56}$$

is satisfied if

$$\left(\sum_{i\in[1,d]} \|f'_i(u)\|_{L^\infty} \right)^{2r} \frac{S_r\, \delta t^{2r}}{\delta x^{2r}} \leq 2C\delta t, \tag{5.57}$$

i.e. condition (5.52).

6 Conclusion

The stability CFL-like conditions presented in this paper may be encountered in many simulations of convection-dominated problems using explicit numerical schemes. Although these stability criteria can be readily obtained using a classical von Neumann stability analysis, they had not been disclosed until now.

The theoretical part of this work allows us to extend the domain of application of these results to different equations with boundaries, assuming some smoothness properties of the solution. Numerical tests validate our approach and support its correctness.

As we need the solution to be smooth, the frame of application restrains to a rather limited area. Nevertheless, the fact that these results can be demonstrated with elementary mathematics and lead to clear and accurate stability conditions makes our work accessible to a wide community, in particular to those who perform numerical simulations of turbulent flows with spectral codes.

Acknowledgements

E.D. gratefully acknowledges the CEMRACS 2007 organizers for his stay in the CIRM in Marseilles and for his access to its rich bibliographical resources, as well as Institute of Fundamental Technological Research Polish Academy of Sciences (IPPT PAN) and Commissariat l'Énergie Atomique (CEA) for his stays there. E.D. also wishes to express his gratitude to Yvon Maday and Frédéric Coquel for fruitful discussions. The authors are grateful to Kai Schneider for graciously providing part of the simulation code and enlightening discussions.

References

[1] P. Angot, C.H. Bruneau, P. Fabrie, *A penalisation method to take into account obstacles in viscous flows.* Numer. Math. **81**, 497–520, 1999.

[2] C. Canuto, M.T. Hussaini, A. Quarteroni, and T.A. Zang, *Spectral methods in fluid dynamics*, Springer-Verlag, New-York, 1988.

[3] J.G. Charney, R. Fjörtoft, J. von Neumann, *Numerical Integration of the Barotropic Vorticity Equation*, Tellus, **2** 237–254, 1950.

[4] B. Cockburn, C.-W. Shu *Runge-Kutta discontinuous Galerkin methods for convection-dominated problems*, J. Sci. Comput. **16** 173–261, 2001.

[5] R. Courant, K. Friedrichs, H. Lewy, *On the Partial Difference Equations of Mathematical Physics*, IBM Journal, march 1967, translation from a paper originally appeared in *Mathematische Annalen* **100** 32–74, 1928.

[6] E. Deriaz and V. Perrier, *Direct Numerical Simulation of turbulence using divergence-free wavelets*, E. Deriaz et V. Perrier, SIAM Multiscale Modeling and Simulation **7**(3) 1101–1129, 2008.

[7] D. Levy and E. Tadmor, *From Semidiscrete to Fully Discrete: Stability of Runge–Kutta Schemes by The Energy Method*, SIAM Review, **40**(1) 40–73, 1998.

[8] R. Kupferman and E. Tadmor, *A fast, high resolution, second-order central scheme for incompressible flows*, Proc. Natl. Acad. Sci. USA Vol. 94, pp. 4848-4852, May 1997 Mathematics.

[9] M. Marion and R. Temam, Handbook of Numerical Analysis, Vol. VI, *Numerical Methods for Fluids* (Part 1), Elsevier Science, 1998.

[10] R. Peyret, *Handbook of computational fluid mechanics*, Academic Press, 2000.

[11] K. Schneider. *Numerical simulation of the transient flow behaviour in chemical reactors using a penalization method.* Computers & Fluids, 34, pp. 1223-1238 (2005).

[12] V. Girault, P.A. Raviart, *Finite element methods for Navier-Stokes equations*, Springer-Verlag Berlin, 1986.

[13] D. Gottlieb and E. Tadmor, *The CFL condition for spectral approximations to hyperbolic initial-boundary value problems*, Mathematics of Computation **56**(194): 565-588, 1991.

[14] R. Temam, *The Navier-Stokes equations*, North-Holland, Amsterdam, 1984.

[15] L. N. Trefethen, *Finite Difference and Spectral Methods*, book not published, available on the author's webpage, 1994.

[16] K. Urban, *Wavelet Bases in H(div) and H(curl)*, Mathematics of Computation **70**(234): 739-766, 2000.

[17] P. Wesseling, *Principles of Computational Fluid Dynamics*, Berlin et al., Springer-Verlag 2001.

[18] Q. Zhang and C.-W. Shu, *Error Estimates to Smooth Solutions of Runge–Kutta Discontinuous Galerkin Methods for Scalar Conservation Laws*, SIAM J. Numer. Anal. **42**(2): 641–666, 2004.